Electronic Supplementary Information

Insertion reaction of carbon dioxide into Sn-O bond. NMR, crystal structures of di- and tetranuclear isopropoxycarbonato tin(IV) complexes, and DFT calculations

Danielle Ballivet-Tkatchenko,* Henry Chermette, Laurent Plasseraud and Olaf Walter

**LSEO, UMR 5188 CNRS-Université de Bourgogne, UFR Sciences et Techniques, BP 47870, 21078 Dijon Cedex, France; E-mail: ballivet@u-bourgogne.fr*

Supporting Information

NMR and IR spectra

The ^{1}H, $^{119}Sn\{^{1}H\}$, and ^{13}C NMR experiments were run on a Bruker Avance 300 spectrometer at 300.131, 111.910, and 75.475 MHz, respectively; *J* values are given in Hz. ^{1}H and ^{13}C chemical shifts (δ, ppm) were determined relative to the solvent (^{1}H, $CHCl_3$, δ 7.24; $CDCl_3$, δ 77.00) and converted to the scale downfield from Me_4Si. $^{119}Sn\{^{1}H\}$ chemical shifts (δ, ppm) are reported downfield from Me_4Sn, as the internal standard. IR spectra were recorded on a Bruker Vector 22 equipped with a Specac Golden Gate^{TM} ATR device.

Figure 1.
ATR IR spectra of neat *n*-$Bu_2Sn(O^iPr)_2$ (**1**) before and after reaction with CO_2

Figure 2.
ATR IR spectra of neat [*n*-$Bu_2(^iPrO)Sn]_2O$ (**3**) before and after reaction with CO_2

Figure 3.
^{1}H, $^{119}Sn\{^{1}H\}$, $^{13}C\{^{1}H\}$, and ^{13}C DEPT-135 NMR of *n*-$Bu_2Sn(O^iPr)_2$ (**1**) at 295 K

Figure 4.
^{1}H, $^{119}Sn\{^{1}H\}$, $^{13}C\{^{1}H\}$, and ^{13}C DEPT-135 NMR of *n*-$Bu_2Sn(O^iPr)(OCO_2{}^iPr)$ (**2**) at 253 K

Figure 5.
^{1}H, $^{119}Sn\{^{1}H\}$, $^{13}C\{^{1}H\}$, and ^{13}C DEPT-135 NMR of [*n*-$Bu_2(O^iPr)Sn]_2O$ (**3**) at 295 K

Figure 6.
^{1}H, $^{119}Sn\{^{1}H\}$, $^{13}C\{^{1}H\}$, and ^{13}C DEPT-135 NMR of *n*-$Bu_2(^iPrO)SnOSn(OCO_2{}^iPr)$*n*-$Bu_2$(**4**) at 295 K

Figure 7.
^{13}C DEPT-135 and ^{1}H NMR of *n*-$Bu_2Sn(O^iPr)(O^{13}CO_2{}^iPr)$ (**2**) after enrichment with labelled $^{13}CO_2$

Figure 8.
$^{119}Sn\{^{1}H\}$ and $^{13}C\{^{1}H\}$ NMR of *n*-$Bu_2Sn(O^iPr)(O^{13}CO_2{}^iPr)$ (**4**) after enrichment with labelled $^{13}CO_2$

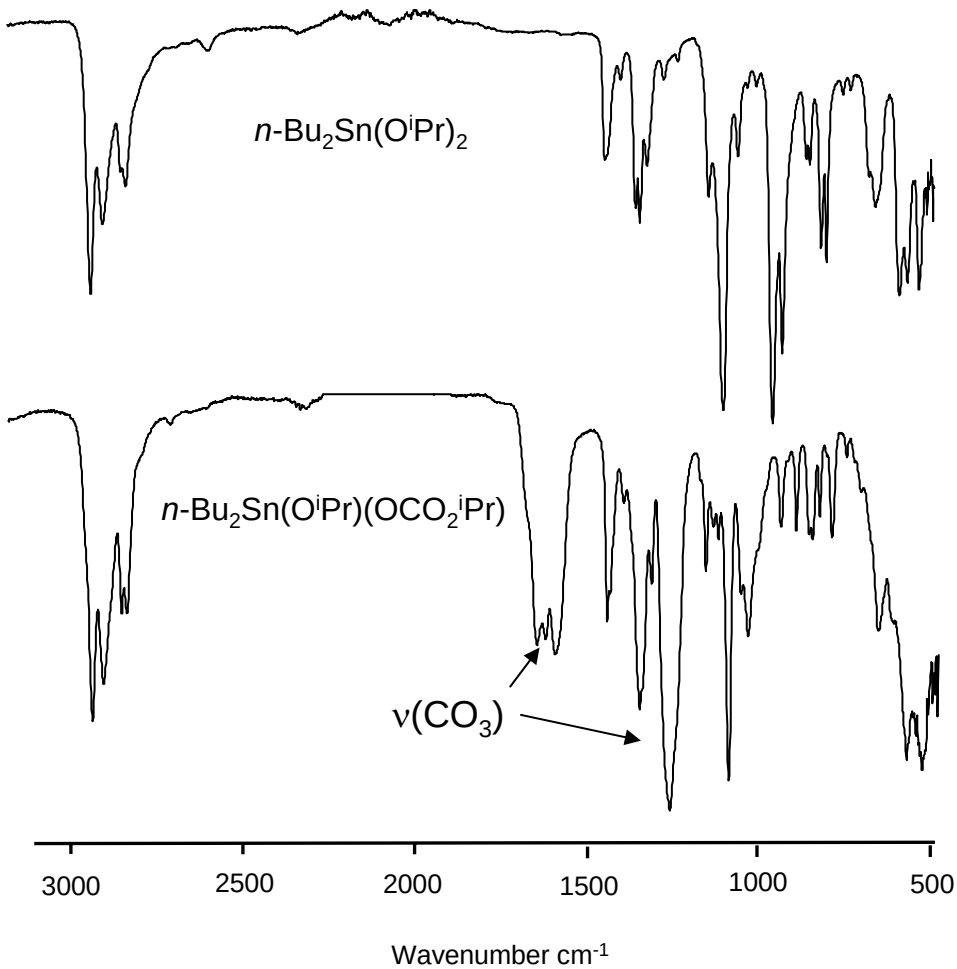

Figure 1.
ATR IR spectra of neat *n*-$Bu_2Sn(O^iPr)_2$ (**1**) before and after reaction with CO_2

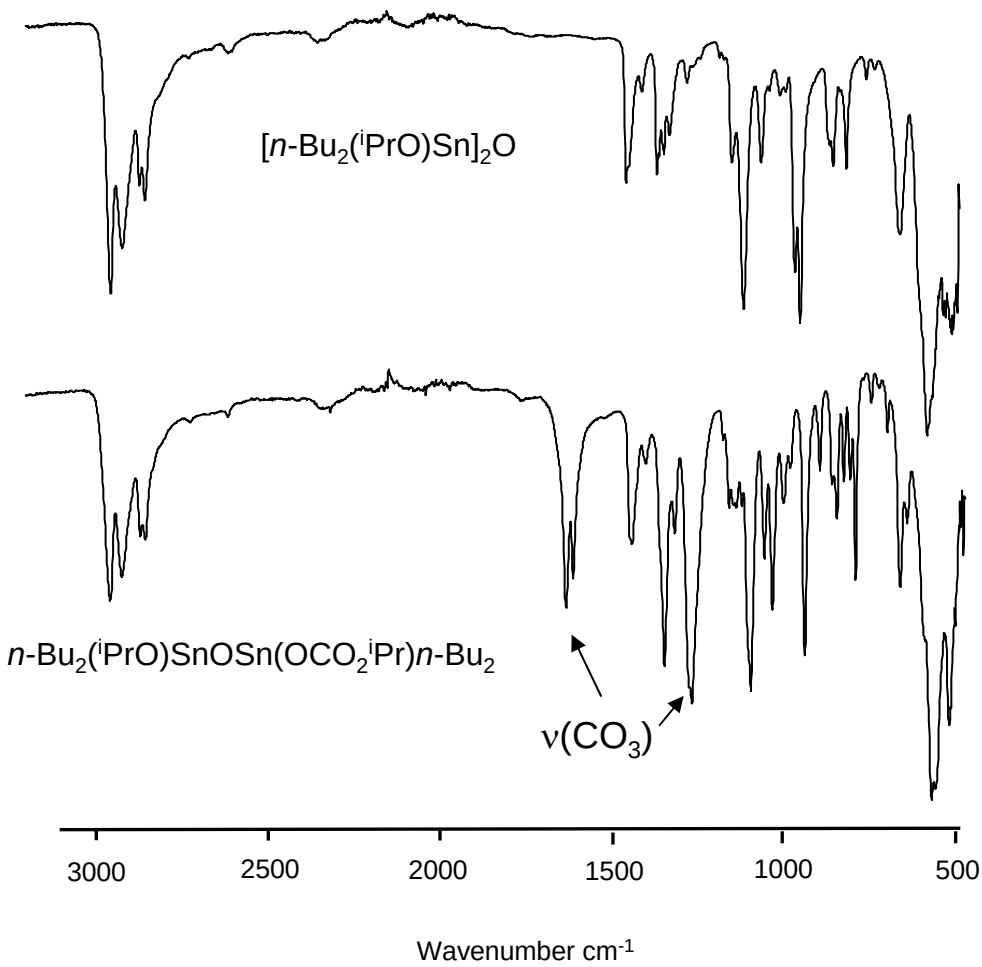

Figure 2.
ATR IR spectra of neat [*n*-Bu_2(^{i}PrO)Sn]$_2$O (**3**) before and after reaction with CO_2

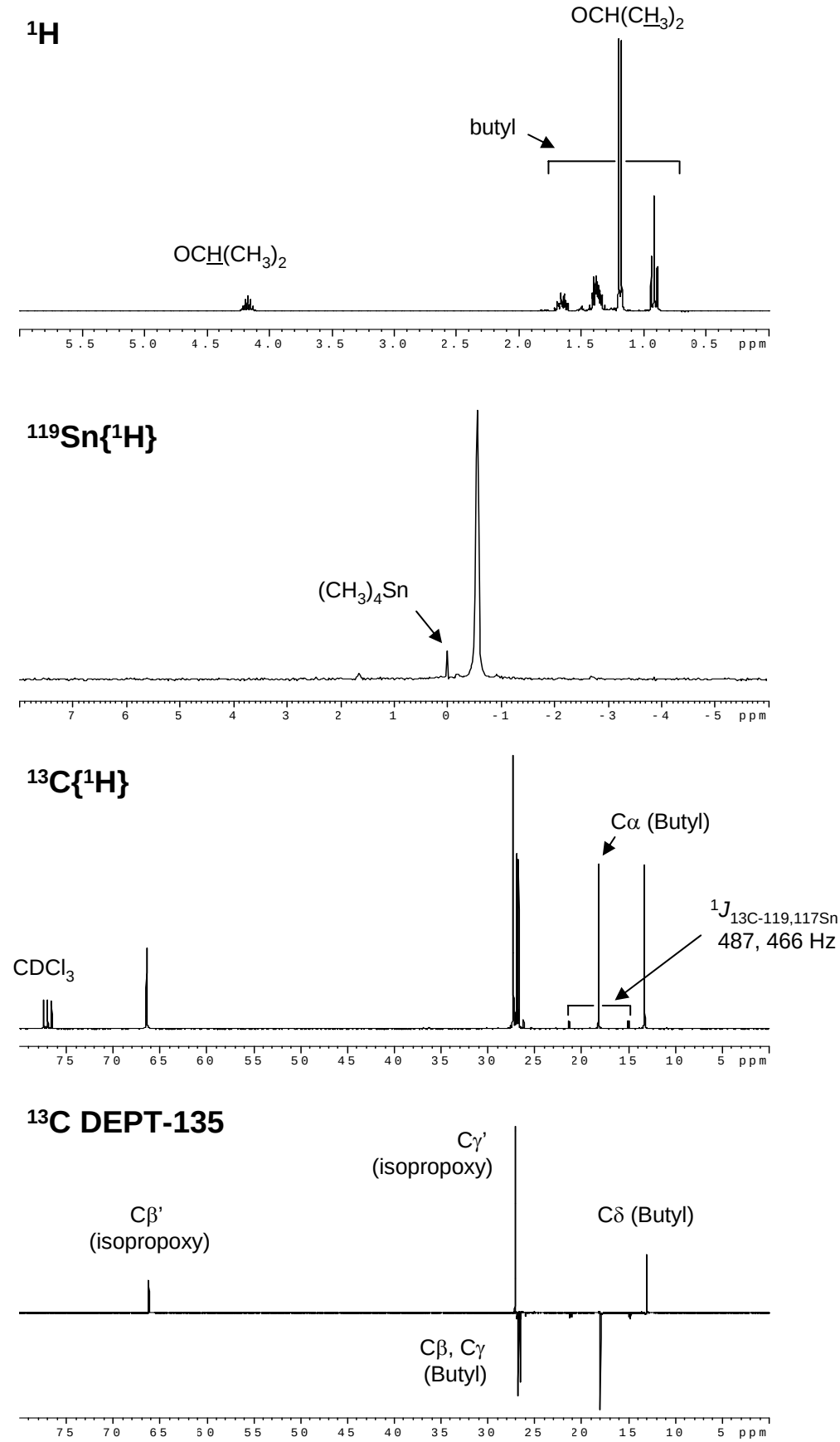

Figure 3.

^{1}H, $^{119}Sn\{^{1}H\}$, $^{13}C\{^{1}H\}$, and ^{13}C DEPT-135 NMR of *n*-$Bu_2Sn(O^iPr)_2$ (**1**) at 295 K

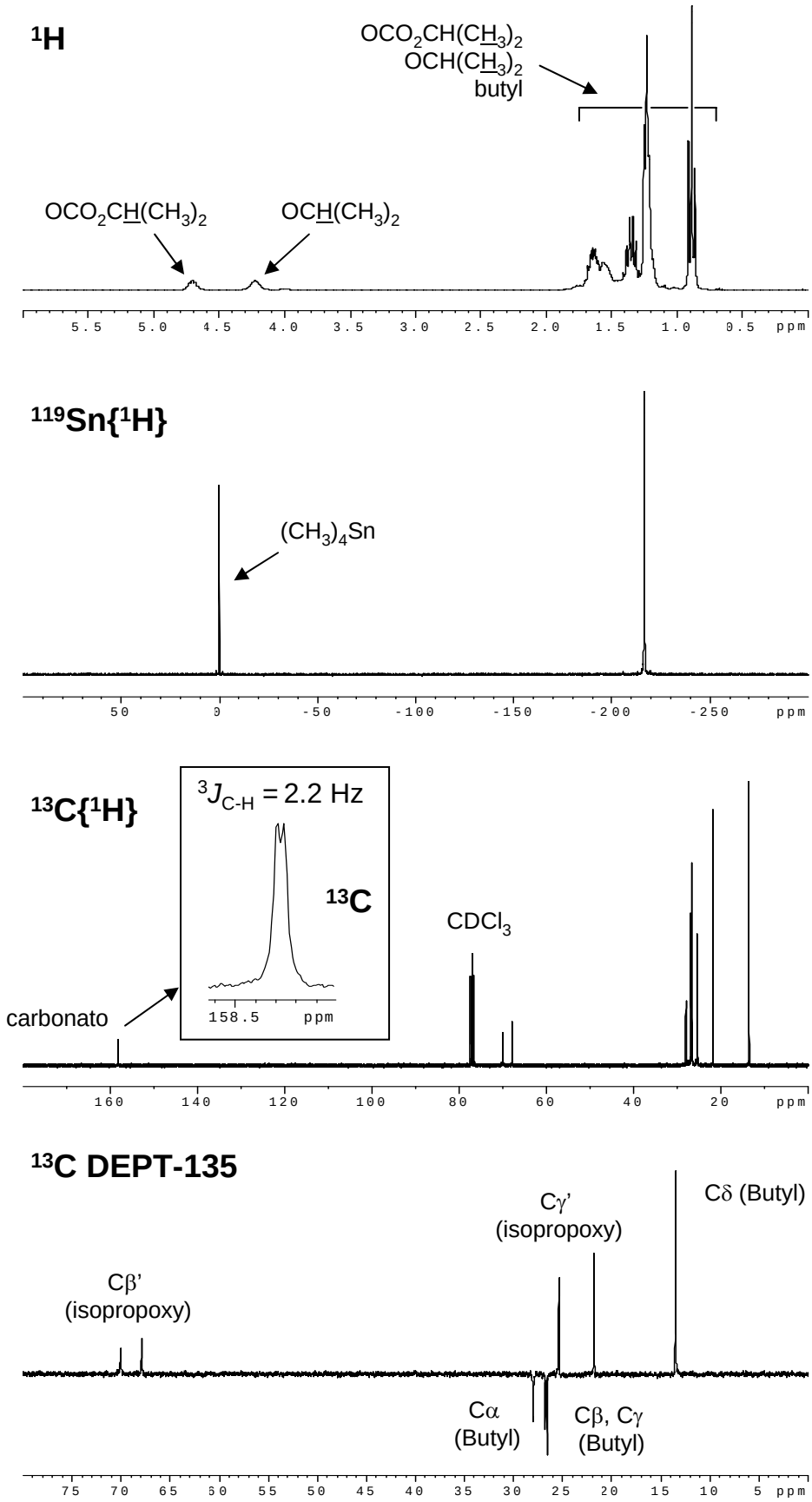

Figure 4.

^{1}H, ^{119}Sn{^{1}H}, ^{13}C{^{1}H}, and ^{13}C DEPT-135 NMR of *n*-$Bu_2Sn(O^iPr)(OCO_2{}^iPr)$ (**2**) at 253 K

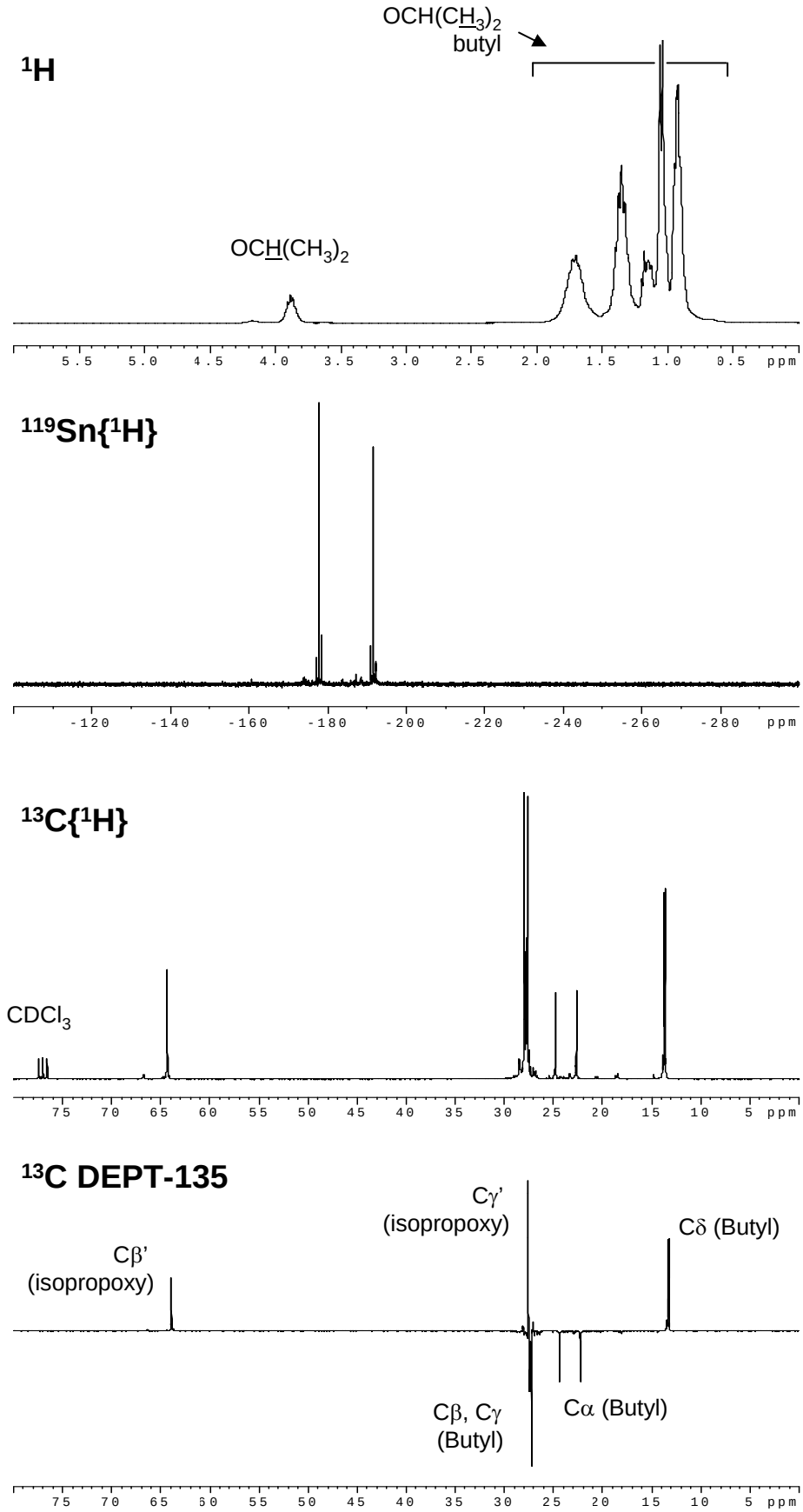

Figure 5.

^{1}H, ^{119}Sn{^{1}H}, ^{13}C{^{1}H}, and ^{13}C DEPT-135 NMR of [*n*-Bu$_2$(O^{i}Pr)Sn]$_2$O (**3**) at 295 K

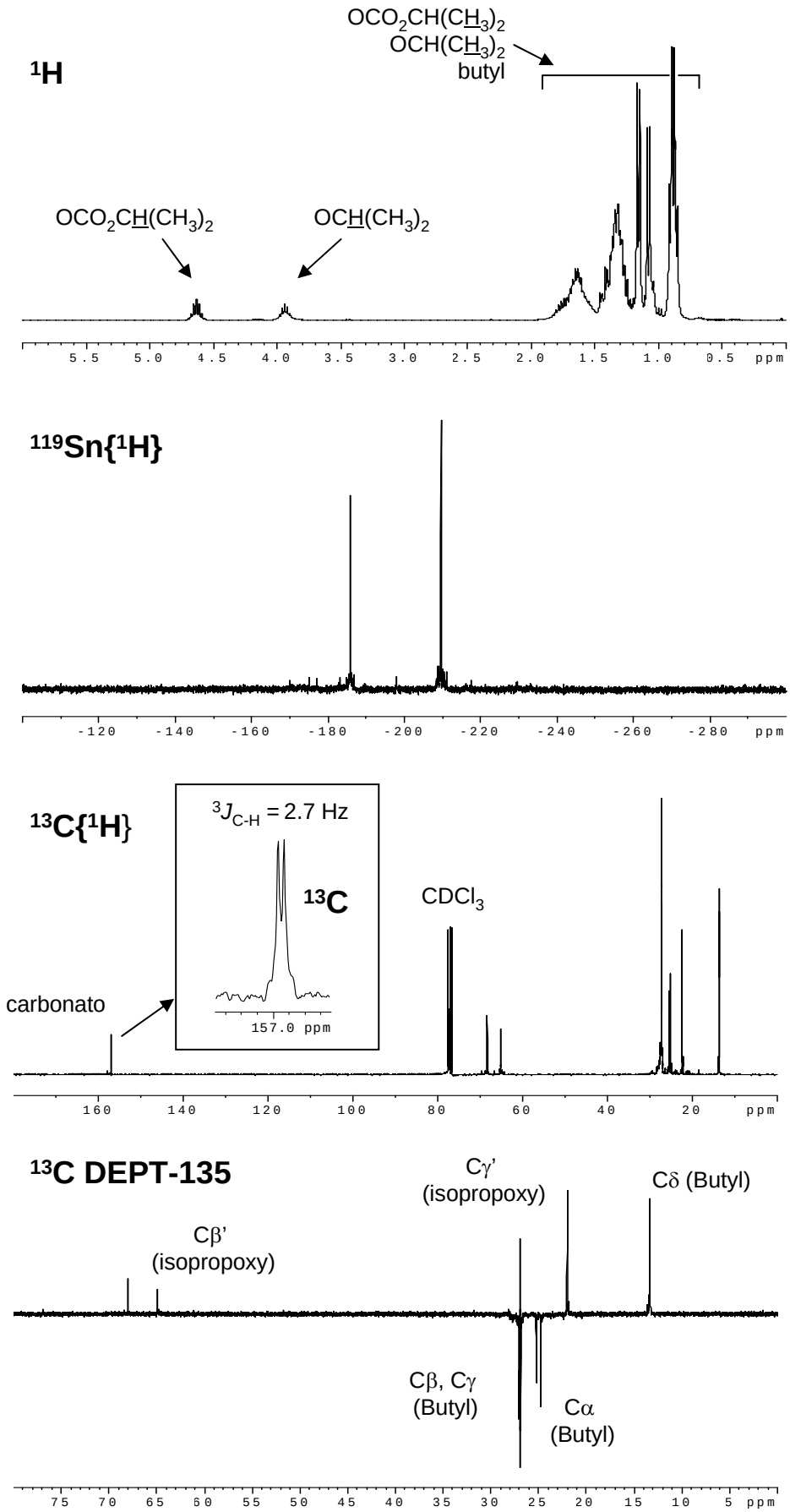

Figure 6.

^{1}H, ^{119}Sn{^{1}H}, ^{13}C{^{1}H}, and ^{13}C DEPT-135 NMR of *n*-Bu_2(^{i}PrO)SnOSn($OCO_2{}^{i}$Pr)*n*-Bu_2(**4**) at 295 K

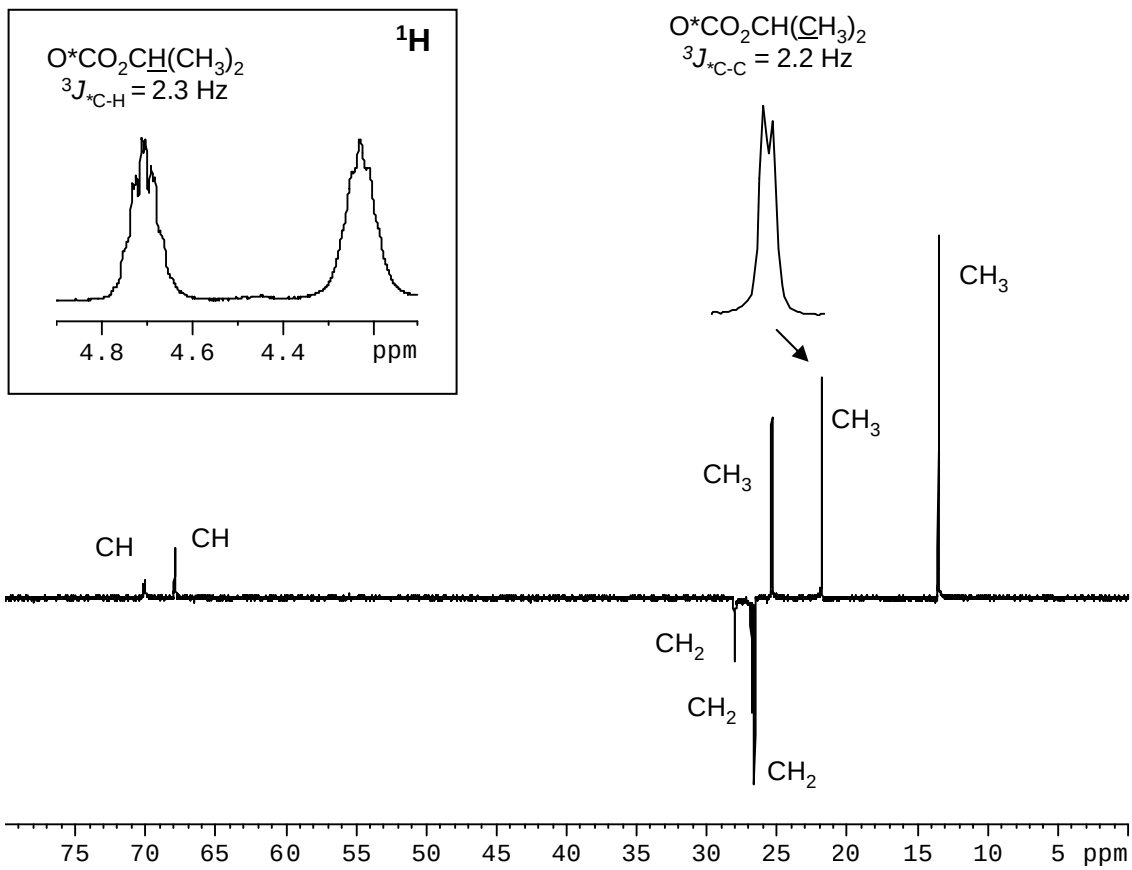

Figure 7.

^{13}C DEPT-135 and ^{1}H NMR of *n*-Bu$_2$Sn(O^{i}Pr)(O^{13}CO$_2{}^i$Pr) (**2**) after enrichment with labelled $^{13}CO_2$

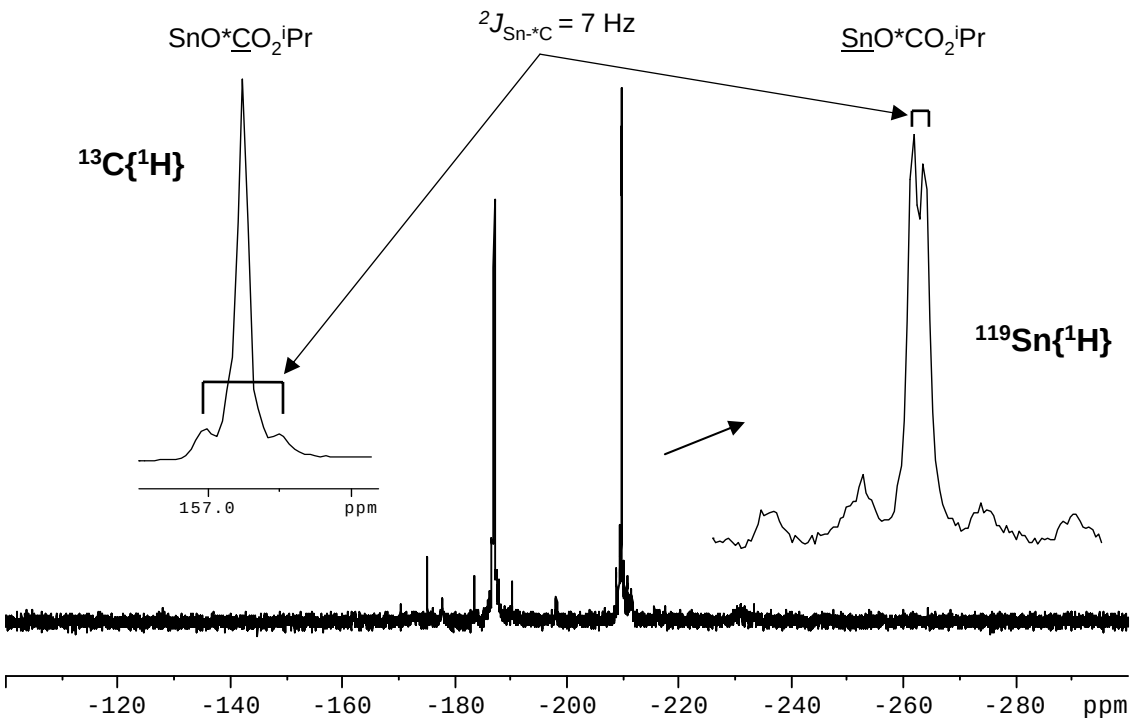

Figure 8.

$^{119}Sn\{^{1}H\}$ and $^{13}C\{^{1}H\}$ NMR of *n*-$Bu_2Sn(O^iPr)(O^{13}CO_2{}^iPr)$ (**4**) after enrichment with labelled $^{13}CO_2$